



Rebound in China's coastal wetlands following conservation and restoration

Xinxin Wang^{1,2}, Xiangming Xiao²✉, Xiao Xu¹, Zhenhua Zou³, Bangqian Chen⁴, Yuanwei Qin², Xi Zhang¹, Jinwei Dong⁵, Diyou Liu⁶, Lianghao Pan^{1,7} and Bo Li^{1,7}✉

The coastal zone of China has experienced large increases in population, economy and urbanization since the early 1980s. Many studies have reported the loss, degradation and fragmentation of coastal wetlands in China at local to regional scales. To date, at the national scale, our knowledge of the spatial distribution, inter-annual variation and multi-decadal trends of coastal wetlands in China remains very limited. Here we analysed ~62,000 Landsat-5, -7 and -8 images over the period 1984–2018 and generated maps of coastal wetlands for individual years in China at 30-m spatial resolution. We found that coastal wetland area significantly decreased between 1984 and 2011. We also found a substantial increase in saltmarsh area and a stable trend of tidal flat area since 2012, driven by reduced anthropogenic activities and increased conservation and restoration efforts. These coastal wetland maps for the period 1984–2018 are invaluable for improvement of coastal wetland management and sustainability in China.

Coastal wetlands serve as natural transitions from land to oceans, and are among the most productive and dynamic ecosystems on Earth due to strong interactions between land-based fluvial processes and coastal oceans^{1,2}. In addition to serving as habitats for wildlife, they provide important ecosystem services for humans, such as protection against storms, food production and pollutant absorption^{1–3}. However, coastal wetlands are under intense pressure from sea level rise⁴, coastal erosion^{2,3}, land reclamation⁵, invasive species⁶ and reduced sediment discharges from major rivers^{4,7}. In developing countries like China, a number of anthropogenic and environmental factors associated with rapid population growth and economic development have threatened coastal wetlands⁸. China lost 50% of its coastal wetlands between 1950 and 2000, at an average rate of 24,000 ha yr⁻¹, due to reclamation¹, which greatly threatens the ecological security of coastal regions. However, owing to the difficulties in mapping coastal wetlands at a large scale, geospatial data on the spatial distribution, inter-annual variation and multi-decadal trends of coastal wetlands and their driving factors over the past three decades in China have not yet been fully investigated.

National-scale data on the spatial distribution of coastal wetlands in China are needed, but existing maps and datasets on coastal wetlands in China were developed either for a specific year or at coarse spatial resolution^{9–12}, which preclude us from tracking the spatio-temporal dynamics of coastal wetlands at a multi-decadal scale³. Recently, a few global datasets for coastal wetlands have become available, such as the global saltmarsh map¹³, mangrove maps¹⁴ and tidal flat dataset², but these relate only to specific subtypes of coastal wetlands. Most remote-sensing studies on coastal wetlands in China have been conducted at local and regional scales^{10–12,15}, and some of those studies reported on specific sub-

types of coastal wetlands such as saltmarshes^{16,17}, mangroves^{18–20} or tidal flats^{3,21}. These maps are not sufficient for understanding the long-term dynamics of coastal wetlands (including tidal flats, saltmarshes and mangrove forests) in China. Therefore, there is a need to develop annual maps of coastal wetlands from the mid-1980s at high spatial resolution (tens of metres) that can be used not only to quantify the annual dynamics of coastal wetlands but also to assess the impacts of various driving factors on China's coastal zones since the 1980s.

Here we first used all available Landsat-5/7/8 surface reflectance images for the period 1984–2018 (~62,000 images) in the Google Earth Engine (GEE) cloud computing platform, and pixel- and phenology-based mapping approaches^{12,18}, to generate annual coastal wetland maps for China's coastal zone. In this study, coastal wetlands were defined to include two subgroups (tidal vegetation and tidal flats), with tidal vegetation being further divided into coastal saltmarshes and mangrove forests¹². Second, we analysed the spatial distribution and multi-decadal trends of coastal wetland areas at the 1-km grid cell, deltaic, provincial and national scales. Finally, we assessed the effects of major driving factors (Methods) on the spatio-temporal dynamics of coastal wetlands in China for the period 1984–2018 and discuss their implications for coastal wetland management and sustainability.

Annual maps of coastal wetlands in China in 1984–2018

We generated annual maps of coastal wetlands in China at 30-m spatial resolution for the period 1984–2018 (Supplementary Note 4). Coastal wetlands in China are mainly distributed in regions with low-sloping coastlines, coinciding with large tidal ranges and high sediment inflows (for example, Jiangsu Province) and tide-dominated estuaries and deltas². Figure 1 shows maps of

¹Ministry of Education Key Laboratory for Biodiversity Science and Ecological Engineering, National Observations and Research Station for Wetland Ecosystems of the Yangtze Estuary, Institute of Biodiversity Science and Institute of Eco-Chongming, School of Life Sciences, Fudan University, Shanghai, China. ²Department of Microbiology and Plant Biology, Center for Earth Observation and Modeling, University of Oklahoma, Norman, OK, USA. ³Department of Geographical Sciences, University of Maryland, College Park, MD, USA. ⁴Rubber Research Institute, Chinese Academy of Tropical Agricultural Sciences, Danzhou, China. ⁵Key Laboratory of Land Surface Pattern and Simulation, Institute of Geographic Sciences and Natural Resources Research, Chinese Academy of Sciences, Beijing, China. ⁶Department of Geographic Information Engineering, College of Land Science and Technology, China Agricultural University, Beijing, China. ⁷Guangxi Key Lab of Mangrove Conservation and Utilization, Guangxi Mangrove Research Center, Guangxi Academy of Sciences, Beihai, China. ✉e-mail: xiangming.xiao@ou.edu; bool@fudan.edu.cn

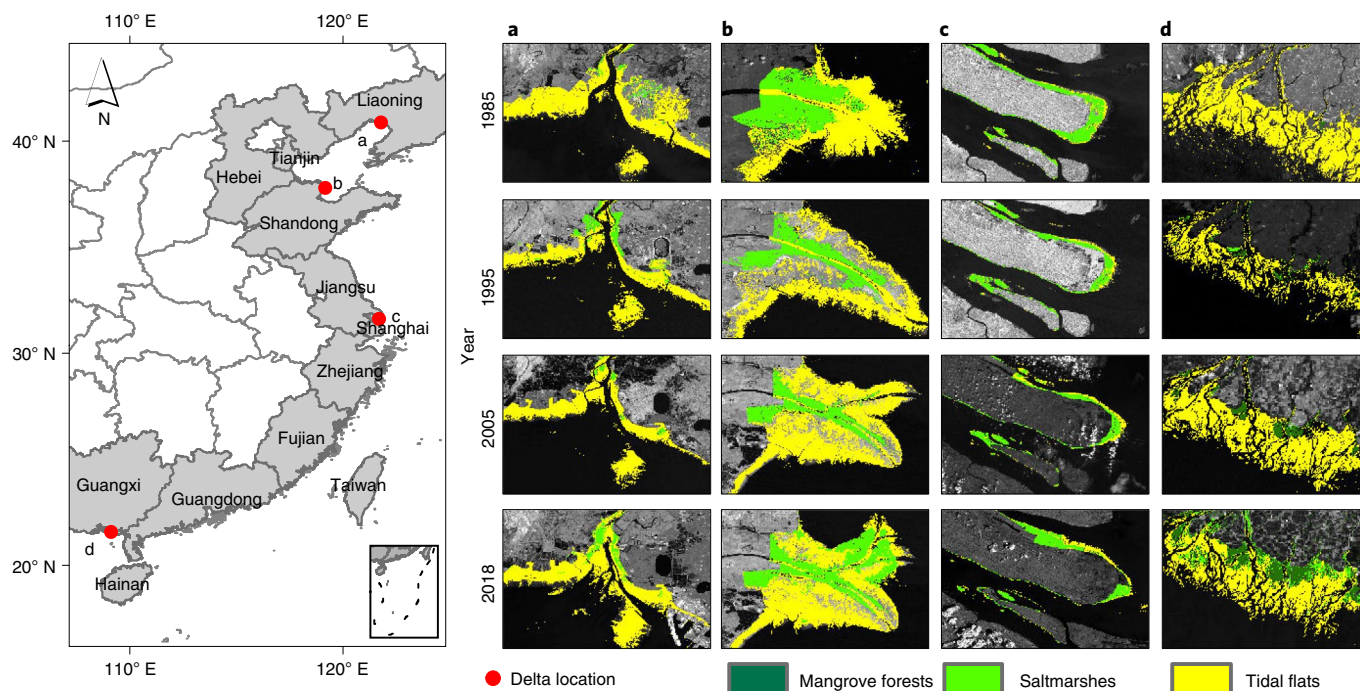


Fig. 1 | Maps of coastal wetlands in four river deltas of China: 1985, 1995, 2005 and 2018. a, Liaohe River delta in Liaoning (121° 47' 36" E, 40° 52' N). **b,** Yellow River delta in Shandong (119° 15' 39" E, 37° 44' N). **c,** Yangtze delta in Shanghai (121° 57' 40" E, 31° 29' 47" N). **d,** Nanliu River delta in Guangxi (109° 02' 30" E, 21° 35' 38" N).

coastal wetlands in four typical, tide-dominated river deltas for the years 1985, 1995, 2005 and 2018. These maps illustrate the spatial distribution and multi-decadal changes in coastal wetlands—for example, the change in direction of the Yellow River estuary from southeast to northeast (Fig. 1b) and the reclamation on Chongming island in the Yangtze delta (Fig. 1c). The validation results show that our dataset agrees well with recent maps derived from the analysis of Landsat images (Supplementary Note 5), which clearly demonstrates the potential value for analysis of coastal wetland dynamics at annual temporal resolution.

Coastal wetland losses and gains in the major river deltas

The Yellow River delta (YRD) discharges the largest amount of mud and sand into the river²² and is the largest and most dynamic delta in China. Geographically, inter-annual trends of coastal wetland areas in the YRD within individual 1-km gridcells (Fig. 2a–c) show that the new northeastern mouth of the Yellow River experienced significant gains in both tidal flats and saltmarshes between 1984 and 2018; however, other regions experienced considerable losses in terms of tidal flats and saltmarshes, especially in the northern and southern YRD, as well as the old southeastern mouth of the Yellow River²³ (Supplementary Fig. 1). Coastal wetland areas in the YRD decreased significantly between 1984 and 2018 (Fig. 2d). However, a significantly increased area of saltmarsh between 2011 and 2018 (slope, $10.0 \pm 5.29 \text{ km}^2 \text{ yr}^{-1}$) was found in our study, indicating recovery of saltmarshes in the YRD since 2011.

The Yangtze Delta (YTD) is home to 30% of China's population and ranks top among regional economies. Coastal wetlands in Shanghai municipality underwent many changes due to both reduced sediment load and human activities²⁴. The inter-annual trends for coastal wetland areas within individual 1-km grid cells between 1984 and 2018 (Fig. 2e–g) show large spatial variation. Substantial losses of coastal wetland areas were found on Chongming island and southern Shanghai (Lingang New City) (Supplementary Fig. 2), and substantial gains in coastal wetland areas were found on

Changxing and Jiuduansha islands. The inter-annual trends of total tidal flat and saltmarsh area in the YTD show two-phase dynamics (Fig. 2h): a decreasing phase between 1984 and 1993 and an increasing phase between 1994 and 2018.

The Pearl River delta (PRD) is among the most highly urbanized regions and most developed areas in the world²². Coastal wetlands in the PRD have scattered spatial distribution with small to moderate patch size, and the inter-annual trends for coastal wetlands between 1984 and 2018 were positive in most 1-km grid cells (Fig. 2i–k). Total tidal vegetation area in the PRD increased significantly between 1984 and 2018 (Fig. 2l), although its two subtypes (saltmarshes and mangrove forests) showed different trends (Supplementary Fig. 3). Saltmarsh area was relatively stable ($P > 0.05$) but mangrove forest area showed a significantly increasing trend between 2000 and 2018. After exclusion of high values in 1988 and 2015 (outliers), total tidal flat area in the PRD showed no significant inter-annual trend between 1984 and 2018 (Fig. 2l).

Coastal wetland losses and gains at the provincial scale

Coastal wetlands are distributed unevenly across coastal provinces in China (Supplementary Fig. 4). China had 7,400 km² of coastal wetlands in 2018, including 5,300 km² of tidal flats (72%) and 2,100 km² of tidal vegetation (28%). The tidal flat area in Jiangsu Province, southern China, accounted for 23.9% of the total tidal flat area in China in 2018, followed by that in Shandong Province (15.0%). The tidal vegetation area in Jiangsu was 393 km², accounting for 18.7% of the total tidal vegetation area (2,102 km²) in China, followed by that in Shanghai (18.4%). In total, the coastal wetland area in Jiangsu accounted for 22.4% of the total coastal wetland area in China, followed by that in Shandong (13.8%). In 2018, all mangrove forests were found in southern China^{18,20} with Guangdong having the largest area (41.7%), followed by Guangxi (32.7%).

Coastal wetland areas in individual provinces in China showed remarkably divergent trends between 1984 and 2018 (Fig. 3). Seven provinces experienced significant decreases in tidal flat areas

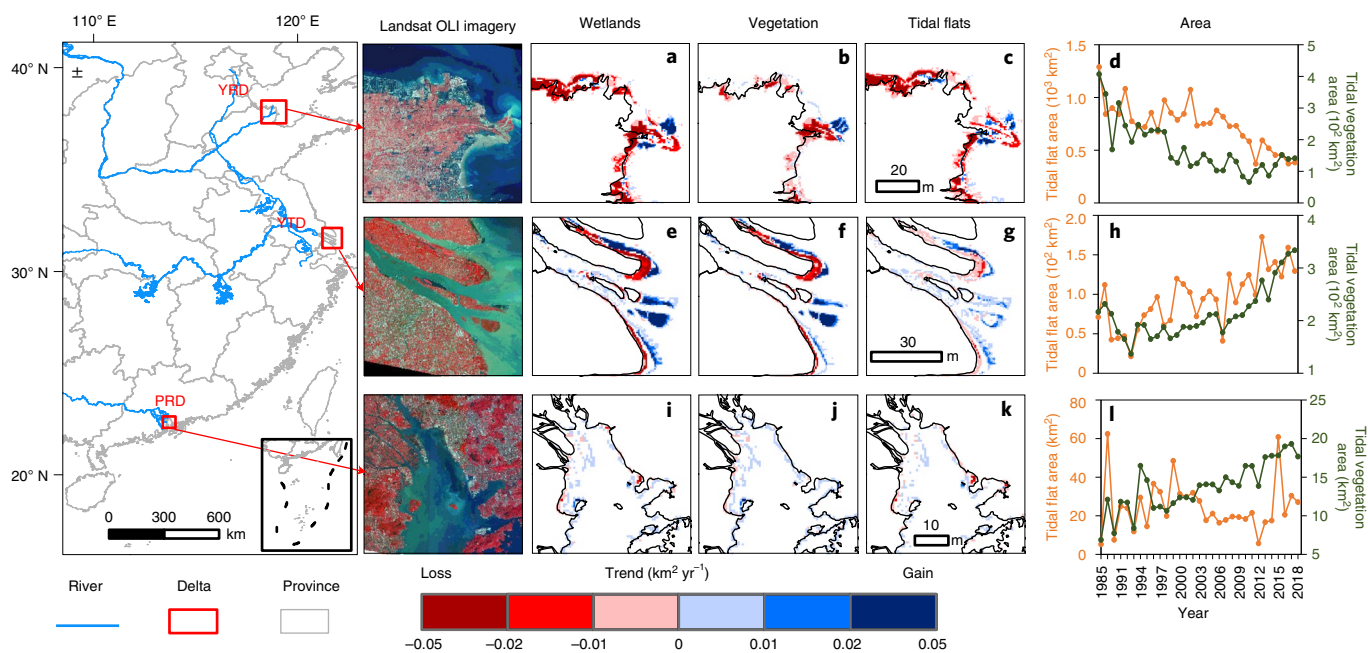


Fig. 2 | Coastal wetland losses and gains in three major Chinese river deltas, 1984–2018. **a–c**, Coastal wetlands (**a**), vegetation (**b**) and tidal flats (**c**) in the YRD at 1-km grid cell scale. **d**, Coastal wetland areas in the YRD. **e–g**, Coastal wetlands (**e**), vegetation (**f**) and tidal flats (**g**) in the YTD at 1-km grid cell scale. **h**, Coastal wetland areas in the YTD. **i–k**, Coastal wetlands (**i**), vegetation (**j**) and tidal flats (**k**) in the PRD at 1-km grid cell scale. **l**, Coastal wetland areas in the PRD. OLI, Operational Land Imager.

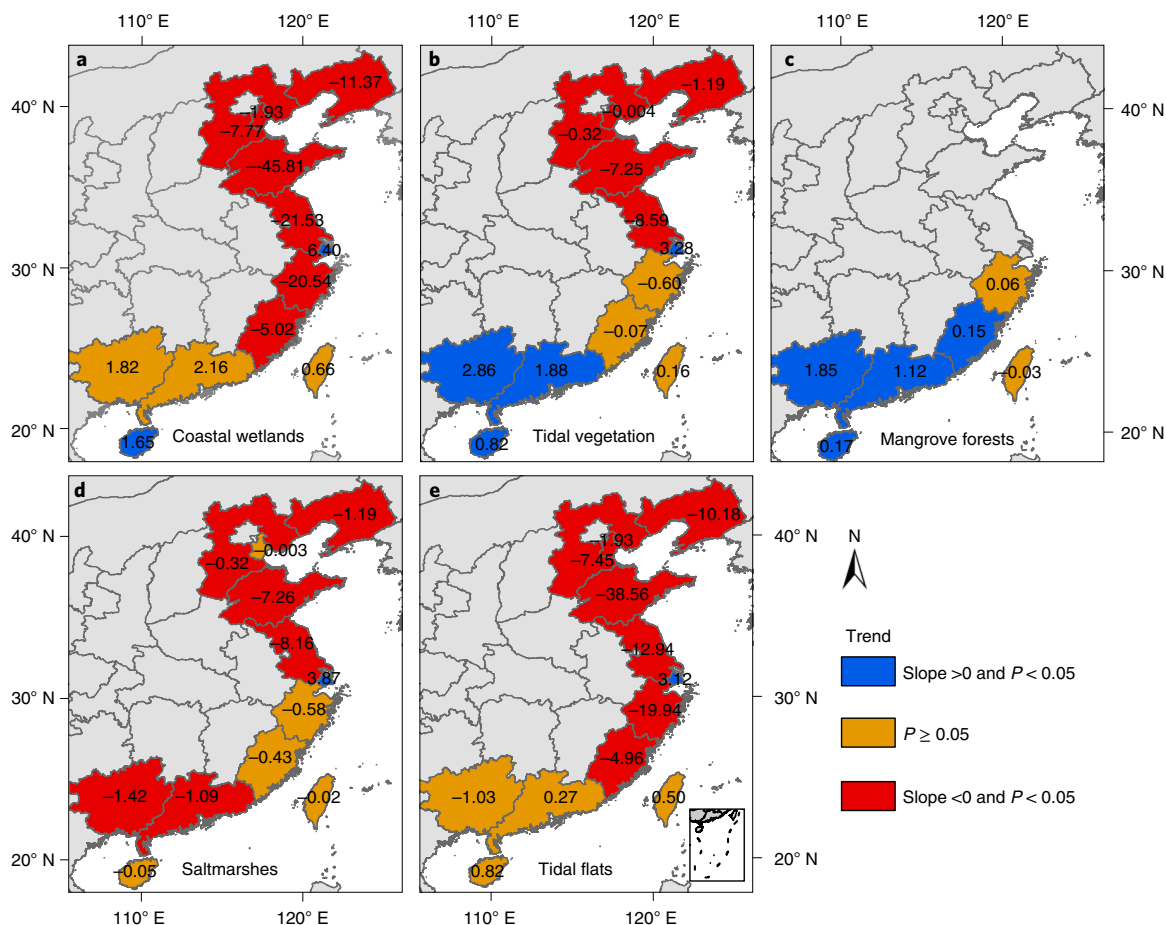


Fig. 3 | Inter-annual trends for coastal wetland areas by province in China, 1984–2018. **a**, Coastal wetlands. **b**, Tidal vegetation. **c**, Mangrove forests. **d**, Saltmarshes. **e**, Tidal flats. Numbers in coloured areas denote coefficient values.

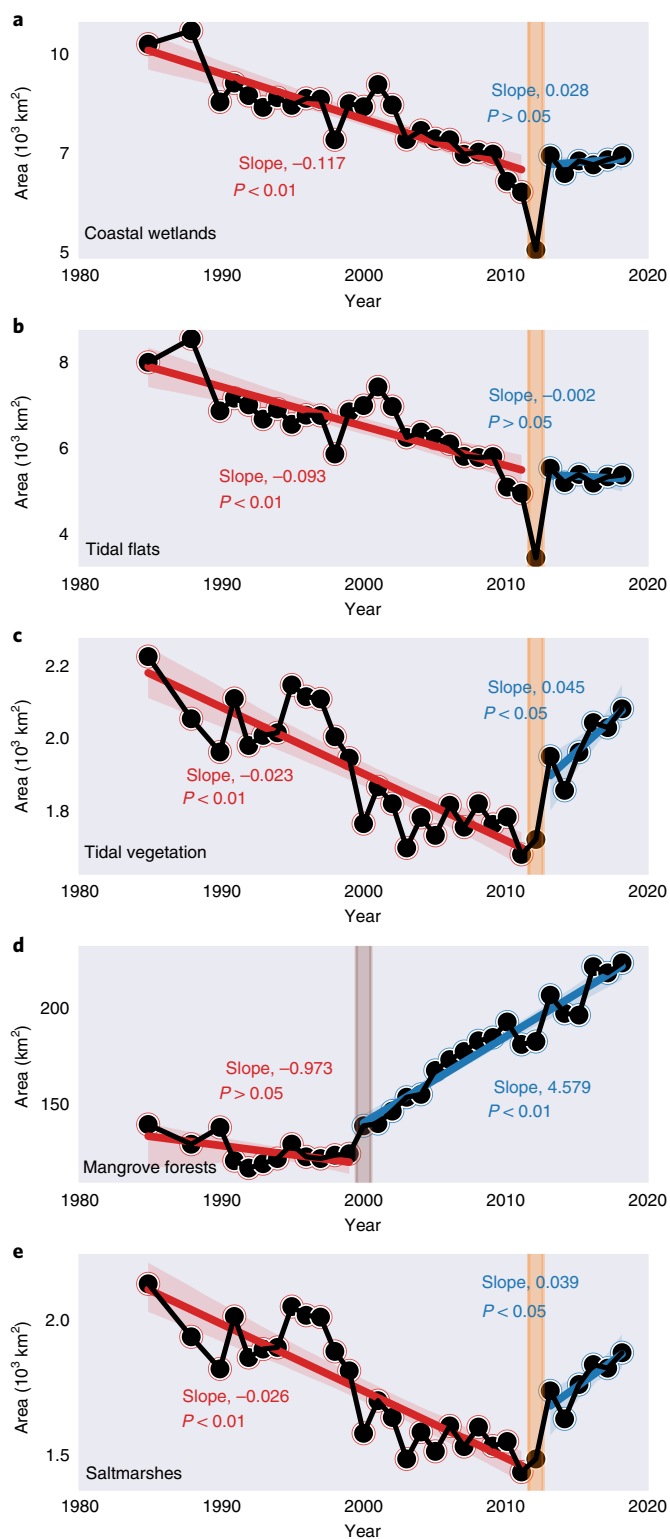


Fig. 4 | Inter-annual changes for coastal wetland areas in China, 1984–2018. **a**, Coastal wetlands. **b**, Tidal flats. **c**, Tidal vegetation. **d**, Mangrove forests. **e**, Saltmarshes. Trends for coastal wetlands, tidal vegetation, saltmarshes and tidal flats in the first and second phases were calculated for 1984–2011 and 2013–2018 (excluding data from 2012), respectively.

(Fig. 3e), with only Shanghai experiencing a significant increase. Compared with tidal flats, the trend for tidal vegetation area significantly decreased in all four provinces in northern China (Fig. 3b),

the rate of decrease in tidal vegetation area being highest in Jiangsu Province. Four provinces in southern China experienced significant increases in area of both tidal vegetation and mangrove forest (Fig. 3c). Coastal wetland areas experienced significant decreases between 1984 and 2018 in all seven provinces located to the north of Guangdong Province, except Shanghai municipality (Fig. 3a). In contrast, only Hainan and Shanghai experienced significant increases in coastal wetland areas (Fig. 3a). In general, provinces in northern China experienced losses of both tidal vegetation and tidal flats while those in southern China experienced divergent trends in areas of tidal vegetation (saltmarshes and mangrove forests) and tidal flats. In addition, these provinces made different contributions to coastal wetland dynamics at the national scale (Supplementary Note 6 and Supplementary Fig. 5).

Coastal wetland losses and gains at the national scale

Coastal wetland areas in China underwent divergent inter-annual trends between 1984 and 2018 at the national scale (Fig. 4a). There were $\sim 10,263 \text{ km}^2$ of coastal wetlands in 1984 (a composite of 1984–1986), comprising $7,980 \text{ km}^2$ of tidal flats, $2,143 \text{ km}^2$ of saltmarshes and 140 km^2 of mangrove forests, and there were $\sim 7,400 \text{ km}^2$ of coastal wetlands in 2018, comprising $\sim 5,300 \text{ km}^2$ of tidal flats, $\sim 1,900 \text{ km}^2$ of saltmarshes and $\sim 220 \text{ km}^2$ of mangrove forests. The coastal wetland area was 27.9% higher in 1984 than in 2018, showing a significantly decreasing trend (slope, $-0.13 \pm 0.02 \times 10^3 \text{ km}^2 \text{ yr}^{-1}$) (Fig. 4a). Specifically, the inter-annual trend of coastal wetland area can be divided into two phases: a significantly decreasing phase between 1984 and 2011 and a slightly to moderately, but non-significantly, increasing phase between 2013 and 2018 (excluding data from 2012 because of limited good-quality observation numbers; Methods). Because tidal flats accounted for a much greater proportion of coastal wetlands than tidal vegetation, the inter-annual dynamics of the former between 1984 and 2018 show the same trend as those of coastal wetlands (Fig. 4e). Geographically, among 25,524 coastal wetlands 1-km grid cells in China's coastal zone, 30.0 and 24.5% had significantly decreasing and increasing trends, respectively (Supplementary Fig. 6a).

Tidal vegetation area in 1984 ($2,283 \text{ km}^2$) was 7% higher than in 2018 ($2,120 \text{ km}^2$) (Fig. 4c). Inter-annual trends for tidal vegetation show two distinct phases: (1) a significantly decreasing phase between 1984 and 2011 and (2) a significantly increasing phase between 2013 and 2018. Inter-annual trends for saltmarsh area (Fig. 4d) were similar to those of the tidal vegetation, because saltmarsh area was substantially larger than mangrove forest area (Fig. 4e). In contrast, mangrove forest area shows a three-phase dynamics: (1) a large decreasing phase between 1984 and 1992, (2) a small increasing phase between 1993 and 1999 and (3) a large increasing phase between 2000 and 2018 (Fig. 4e).

Drivers of coastal wetland dynamics in China

A number of case studies at local and deltaic scales have investigated how changes in socioeconomic conditions, policies, climate and sea level rise affect the spatio-temporal dynamics of coastal wetlands^{5,15,22,25}. Their results provide useful information to support the quantitative analyses of various driving factors responsible for the spatio-temporal dynamics of coastal wetlands in China at large spatial scales. Here we used structural equation modelling, multivariate regression models and simple linear regression models for attribution analyses at the scales of river delta, province and nation.

In the YRD, land reclamation and coastal development—such as conversion to aquaculture ponds—were major drivers of tidal flat loss²². Sea water intrusion also accelerated the loss of coastal wetlands in the northern and southern YRD²³. Furthermore, reduced sediment load in the Yellow River was significantly correlated with loss of tidal vegetation²⁶ (Supplementary Fig. 7a,b). In the YTD, multi-phase reclamation and urban construction projects caused

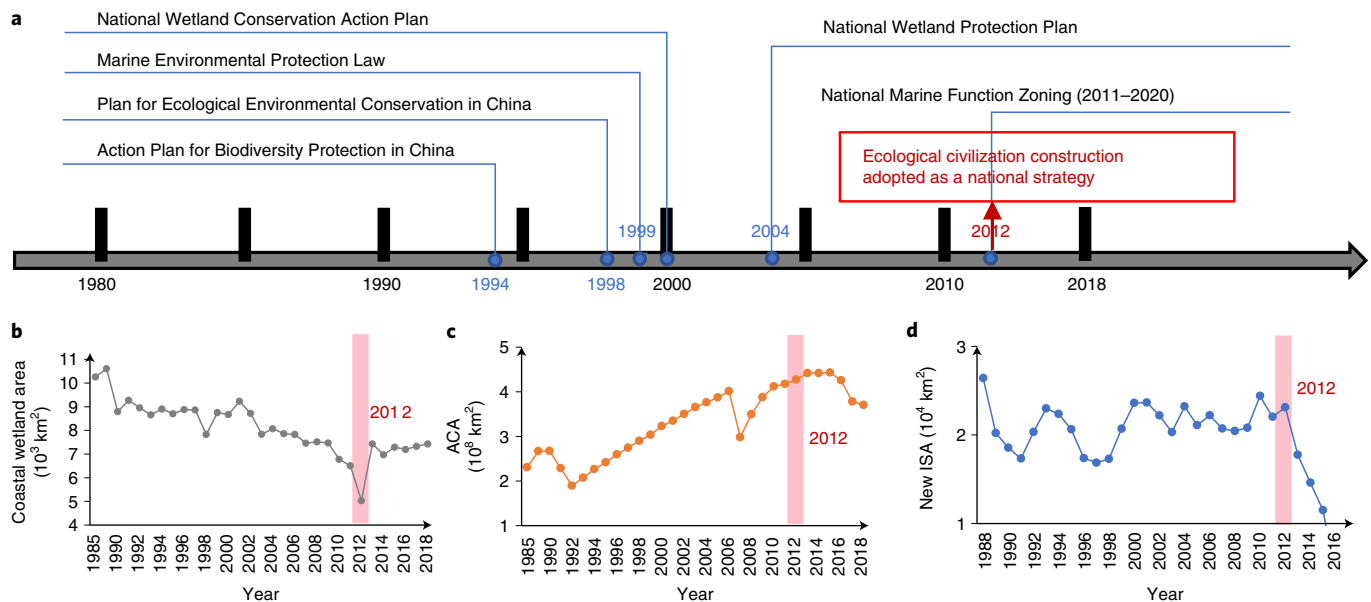


Fig. 5 | Timeline of major policies and laws in regard to wetlands and coastal wetlands and their impacts on inter-annual changes in coastal wetland areas, ACAs and new ISAs in China, 1984–2018. a, Major policies and laws introduced since 1980. b, Coastal wetland areas. c, ACAs. d, New ISAs.

substantial coastal wetland losses on Chongming island and southern Shanghai (Lingang New City)^{27,28} (Supplementary Fig. 2). Substantial coastal wetland gains were found on Changxing and Jiuduansha islands in YTD because of limited human disturbance and expansion of invasive *Spartina alterniflora* saltmarshes¹⁷. In the PRD, urbanization rather than sediment load (Supplementary Fig. 7f) was identified as the primary driver of tidal flat losses since 2000, because urban area increased from 121 km² in 2000 to 324 km² in 2015 (ref. ²⁹). Gains in tidal vegetation area were mainly driven by increase in mangrove forest areas through various conservation and restoration projects implemented by governments^{19,20}. The National Marine Function Zoning Plan (2011–2020)³⁰ also contributed to coastal wetland gains in the PRD from 2012.

At the provincial scale, human activities were the major drivers of inter-annual variation in coastal wetland areas^{31–33}. For the inter-annual dynamics of tidal flat areas, aquaculture area (ACA) was a statistically significant variable for two provinces (Shandong and Guangxi). The negative regression slope for Shandong indicated that increase in ACA contributed to decrease in tidal flat area (Supplementary Table 1). Impervious surface area (ISA) was a statistically significant variable for four provinces, especially those in southern China with negative regression slopes. Population was a statistically significant variable for five provinces. The significant regressions between land use change (for example, ACA and ISA) and socioeconomic factors suggest that increased human activities significantly contributed to losses of tidal flat areas in these provinces³⁴. For the inter-annual dynamics of tidal vegetation, ACA was a statistically significant variable for four provinces (Supplementary Table 2) and the coefficients for Tianjin, Shandong and Guangdong Provinces were negative, indicating the significant contribution of ACA to losses of tidal vegetation area in those provinces³⁴. Increase in ISA had a significantly negative correlation with tidal vegetation area in Liaoning and Guangxi provinces, indicating its contribution to losses of tidal vegetation. Moreover, population increase had a significantly negative correlation with tidal vegetation area in Liaoning and Hebei provinces, indicating the contribution of population pressure to losses of tidal vegetation^{10,35,36}.

At the national scale, population growth was correlated with expansion of ACAs and ISAs, and with increase in average air temperature in China's coastal zone between 1984 and 2018

(Supplementary Fig. 8). Increased ISA, driven by the expansion of urbanization and infrastructure, resulted in substantial loss of tidal flat area (Supplementary Fig. 8a). From simple linear model results we found that ACAs had significantly negative effects on changes in tidal vegetation and tidal flat areas (Supplementary Fig. 9a). Relationships between tidal flat areas and socioeconomic factors (gross domestic product (GDP) and population) could be divided into two phases (Supplementary Fig. 9b,c). In phase 1, tidal flat area decreased significantly as GDP increased, up to approximately 25 trillion ren min bi (RMB) (by 2012) ($P < 0.01$). In phase 2, tidal flats area remained relatively stable while GDP increased from 25.0 to 41.7 trillion RMB ($P > 0.05$) (Supplementary Fig. 9b). In comparison, the relationship between tidal vegetation areas and socioeconomic factors could be divided into three phases (Supplementary Fig. 9b,c). The significant decrease in human activities (reduced rates of growth in both ACA and ISA) in China from 2012 resulted in an increase in coastal wetland area (Fig. 5c,d). Note that, in 2012, 'ecological civilization construction' was adopted as a national strategy, and the State Council of China approved the National Marine Function Zoning Plan (2011–2020) to strengthen the management of reclamation projects and to rationally control the scale of reclamation³⁰ (Fig. 5a). Simultaneously, two national nature reserves were established (Supplementary Fig. 9f and Supplementary Table 3). Reduced anthropogenic disturbances and increased conservation efforts by the government from 2012 contributed to the restoration of coastal wetlands in China.

Discussion

Our study provides strong evidence that there has been substantial loss of coastal wetlands in China. Because coastal wetlands provide diverse important ecosystem goods and services³⁷, their loss has reduced biodiversity, affecting water quality, carbon storage and coastal protection from storm events and increased regional vulnerability to sea level rise which, together, pose threats to human health and coastal sustainability^{1,38,39}. Given the perilous state of coastal wetlands in China and their critical ecosystem services, there is clearly a need for more action to protect and restore coastal wetlands.

Different types of coastal wetlands in China have been subjected to divergent protection strategies. The ecosystem services

of mangrove forests in China were not well recognized in the 1970 and 1980s and, consequently, mangrove forest area has continued to be lost^{19,20}. Since the early 1990s the importance of protecting mangrove forests has been increasingly recognized, and three national mangrove nature reserves have been established in southern and southeastern China²⁰ (Supplementary Table 3), contributing to the small increase in mangrove forest area in the 1990s. By the late 1990s, several large-scale afforestation projects and protection plans began to be implemented to strengthen the conservation of mangrove forests and, accordingly, there have been large increases in mangrove forest area since 2000 (Fig. 4e)—for example, the National Coastal Shelterbelt System Construction Project Plan (2016–2025) was released in 2017, aiming to restore 48,650 ha of mangrove forests in China by 2025.

Although many conservation efforts in China have led to partial recovery of mangrove forests, few national conservation and restoration plans have been introduced for saltmarshes, which are spread across 18,000 km of China's coastline. Only four estuarine national natural reserves have been established to protect estuarine wetland ecosystems, one of these being the YRD Nature Reserve in Shandong Province⁴⁰, which had approximately 524 km² of coastal wetlands in 2018, accounting for only 7% of China's total coastal wetland area. In addition, several regional saltmarsh restoration projects have been carried out since 2012, including the restoration of *Scirpus × mariqueter* saltmarsh in the Yangtze estuary⁴¹, contributing to recent gains of saltmarsh area in China (Fig. 4d). Because these projects cover a very limited range, the conservation of saltmarsh ecosystems still lags far behind that of mangrove forests. Considering the important ecosystem services of these saltmarsh ecosystems, there is an urgent need to put more effort into the protection and restoration of saltmarshes by establishing additional saltmarsh reserves and new saltmarsh protection laws and regulations, and by increasing financial support for saltmarsh research and restoration³⁹.

In addition to mangrove forests, total coastal wetlands in China have also been protected through implementation of environmental laws and regulations since the 1980s (Fig. 5a). The observed losses of coastal wetlands between 1984 and the 2000s (Fig. 4) suggest that these environmental laws and regulations were neither comprehensive nor fully enforced, which led to failure or limited success in halting the decreasing trend in coastal wetlands^{1,39}. Before 2012, human activities—as indicated by ACAs and ISAs, for example,—to increase between 1984 and 2011 (Fig. 5c,d).

China also carried out a number of coastal restoration projects between 1984 and the 2000s in an effort to increase coastal wetland areas, such as a wetland restoration project with an area of 5,024 ha; plant communities quickly re-established after initiation of restoration in 2002 (ref. ⁴²). However, those projects either covered very limited areas or were often poorly enforced and compromised by conflicts with economic development³⁹, and thus the gain in coastal wetlands was much smaller than major losses between 1984 and 2011 at the national scale (Fig. 4). In 2012, ecological civilization was adopted as one of the national development strategies, its key tenets including the need to respect, protect and adapt to nature, environmental restoration and protection and sustainable development. This national development strategy has already had substantial impacts on regional development and sustainability in China^{43,44}, contributing to rapid reductions in aquaculture pond area and new ISAs since 2012 (Fig. 5c,d). Our finding of substantial gains in tidal vegetation area since 2012 (Fig. 4) may represent proof of evidence for the initial success of this national development strategy to reverse the trend of coastal wetland loss. It can be expected that further development of this national strategy, such as establishment of stricter and more systematic laws and regulations, and the banning of destructive economic activities and coastal pollution, could lead to the increasing recovery of coastal wetlands in China.

The protection and restoration of coastal wetlands is the first step towards improving coastal ecosystem services in China. There are still many challenges to restoring the biodiversity, structure and function of coastal wetlands⁴¹. One example is that the range of invasive *S. alterniflora* saltmarshes increased substantially, accounting for ~28% of the increase in saltmarsh area since 2012 (Fig. 4). The rapid and extensive spread of *S. alterniflora* saltmarshes threatened coastal environments by altering estuarine sediment dynamics, outcompeting native plant species and reducing wild bird populations and diversity¹⁷. Therefore, because of the negative impacts of increased area of *S. alterniflora* saltmarshes on coastal ecosystem services, removal of *S. alterniflora* saltmarshes must be considered in the conservation and restoration of coastal wetlands in China¹⁷. Furthermore, ecosystem structures and functions (such as soil carbon sequestration) of restored wetlands remain significantly different from those of natural wetlands⁴⁵, which calls for comprehensive research on the functions of coastal wetlands and how to restore their functions⁴⁶. In summary, to achieve the sustainability of coastal wetlands, China must continue to give top priority to conservation and the restoration of coastal wetlands and their ecosystem services. Our satellite-based mapping tools and resultant maps of coastal wetlands at high spatial resolution (30 m) are important in assessing, monitoring, reporting and verifying future changes in the coastal wetlands of China.

Methods

The work flow of this study comprised five steps: (1) generation of coastal wetland maps in China's coastal zone over the period 1984–2018, using freely available Landsat datasets and pixel- and phenology-based mapping approaches; (2) validation of coastal wetland maps through multiple approaches; (3) exploration of spatial distribution and multi-decadal trends in coastal wetland areas at different scales; (4) analysis of driving factors based on public climate, land use and socioeconomic factors; and (5) discussion of the potential uncertainties and implications for coastal wetland management and sustainability.

Landsat data. We used all available Landsat TM/ETM/OLI surface reflectance (SR) images for China from 1 January 1984 to 31 December 2018 (~62,000 images) in the GEE cloud-processing platform (Supplementary Fig. 10). For each image we used the quality assurance band to identify and remove poor-quality observations, including cloud and cloud shadow. The numbers of Landsat-5, -7 and -8 images in each year were highly variable over the study period (Supplementary Fig. 10a), and there was also large temporal variation in the number of good-quality observations among individual pixels over the study period. Pixels with no good-quality observations accounted for 43.6 and 48.4% of all pixels in 1984 and 1985, respectively (Supplementary Fig. 10b), especially in south China (Supplementary Fig. 11). Furthermore, pixels with more than five good-quality observations within one year accounted for ~49% between 1984 and 1989; however, pixels with no good-quality observations accounted for only 1.1% of all pixels between 1990 and 2018. Because of the limited number of good-quality observations for any year between 1984 and 1989, we generated coastal wetland maps within each 3-year time period (1984–1986 and 1987–1989); for example, we generated maps for 1985 using all Landsat data for the period 1984–1986. This approach, of using 3-year images, enabled us to obtain a larger number of good-quality observations in each of the 3-year periods. For example, pixels with no good-quality observations accounted for approximately 3.0 and 0.91% of all pixels in 1984–1986 and 1987–1989, respectively (Supplementary Figs. 10c and 11c,f). Therefore, in this study we generated two 3-year maps (1985 and 1988) and 29 annual maps of coastal wetlands for the period 1990–2018, for a total of 31 maps.

Available coastal wetland maps and datasets. The Global Intertidal Change Dataset (GICD) represents the first analysis of Landsat images used to determine global tidal flat areas for the period 1984–2016, generated using available Landsat SR images in the GEE platform for 1984–2016 and the random forest algorithm (<https://www.intertidal.app/download>)². The study identified and mapped three classes: tidal flats, permanent water and other (including terrestrial environments and vegetated intertidal systems—for example, marshes and mangroves) and reported tidal flat datasets at 3-year intervals (for example, 2014–2016) at 30-m spatial resolution. We downloaded the GICD for comparison with ours for the same time periods (Supplementary Note 5). We also obtained mangrove forest maps and datasets for China for inter-comparison at the provincial scale. Detailed information about these mangrove forest maps is provided in Supplementary Table 4.

Geospatial datasets of the drivers of coastal wetland dynamics. We grouped drivers into five categories: (1) land-use and land-cover changes, including ACAs

and ISAs associated with urbanization, infrastructure and industrialization; (2) sea level rise; (3) climate, including annual precipitation and annual mean air temperature; (4) socioeconomic factors, including population and GDP; and (5) conservation and restoration efforts, including construction of national nature reserves and government policies and laws (Supplementary Note 7).

1. Land-use and land-cover change data. The ACA data for each province of China in the period 1984–2018 were collected from the China Fishery Statistical Yearbooks (available at <https://data.cnki.net/trade/yearbook/single/n2018120050?z=z009>). The 30-m ISA dataset for China during the same period was collected from a previously published study⁴⁷.
2. Sea level rise data. Data on sea level anomalies from 1984 to 2018 were collected from the China Sea Level Bulletin in 2018 (available at <http://www.mnr.gov.cn/sj/sjfw/hy/gbgg/zghpmgb/>).
3. Climate data. The National Centers for Environmental Prediction-Department of Energy Atmospheric Model Intercomparison Project Reanalysis (R-2), from their website at www.esrl.noaa.gov/psd/, was used to calculate annual precipitation and annual mean air temperature for the period 1984–2018.
4. Socioeconomic data. GDP and human population data in each coastal province of China between 1984 and 2018 were collected from the China Statistical Yearbooks by the National Bureau of Statistics of the People's Republic of China (available at <http://www.stats.gov.cn/tjsj/nds/>).
5. Data on conservation and restoration policies and laws. National nature reserve data for China's coastal regions were collected from a previously published study⁴, and information about restoration policies and laws was collected from multiple resources including published studies^{1,20} and websites.

In addition, we collected data on sediment loads in the YRD, YTD and PRD for the period 1984–2018 from the annual Chinese River Sediment Bulletin (http://www.irtces.org/nszx/cbw/hlmsgb/A550406index_1.htm) to explore their effects on coastal wetland dynamics in the three main deltas.

Coastal wetlands mapping and verification. Differences between water- and vegetation-related indices can be used to identify and map coastal wetlands, including tidal vegetation and non-vegetated tidal flats^{3,12}; two widely used vegetation indices (enhanced vegetation index (EVI) and normalized difference vegetation index (NDVI)) and two water-related spectral indices (land surface water index (LSWI) and modified normalized difference water index (mNDWI)) were calculated from SR data to identify surface water body and green vegetation in this study (Supplementary Note 1). We developed the mNDWI/VIs algorithm, defined as $(mNDWI > NDVI \text{ or } mNDWI > EVI \text{ and } EVI < 0.1)$, to identify and map surface water bodies, which reduces the errors induced by vegetation when it is identified as surface water bodies⁴⁸ (Supplementary Note 2). In addition, we also developed the LWSI/VIs algorithm, defined as $(EVI \geq 0.1, NDVI \geq 0.2 \text{ and } LSWI \geq 0)$, to identify and map green vegetation^{3,12}. By combining the temporal frequencies of surface water bodies and green vegetation over a year, we developed pixel- and phenology-based procedures to identify year-long surface water, tidal vegetation and tidal flats, and we generated annual maps of year-long surface water, tidal vegetation and tidal flats in China using Landsat images¹² (Supplementary Note 3). In addition we developed an algorithm to identify both coastal saltmarshes and mangroves within tidal vegetation¹⁸, and an annual map of mangrove forests in China in 2015 was generated by analysis of time series Landsat and Sentinel-1 images, which have a very high overall accuracy (99%) and kappa coefficient (0.97). In this study, we integrated the mNDWI/VIs and LWSI/VIs algorithms and pixel- and phenology-based procedures to identify open surface water, tidal flats and tidal vegetation (including saltmarshes and mangroves) in China's coastal zone for the period 1984–2018 (Supplementary Fig. 12 and Supplementary Note 4).

The resultant multi-year (1984–1989) and annual (1990–2018) maps were first validated using the stratified random sampling approach (Supplementary Table 5), which is the most popular and robust approach used in accurate assessment of land-cover mapping at different scales, such as global tidal flat datasets³, tidal flat maps and coastal wetland maps^{3,12} and surface water body maps in China⁴⁸ and the contiguous United States⁴⁹ (Supplementary Note 5). These maps were then evaluated using ground reference data on saltmarshes and mangroves in China's coastal zone (Supplementary Table 6) and compared with existing data products in different provinces of China, including the global tidal flat dataset and mangrove maps (Supplementary Note 5 and Supplementary Figs. 13 and 15).

In general, tidal flat areas derived from the GICD were much larger than those from our study by 3-year period and province (Supplementary Fig. 13). One error source is that the GICD classified most (if not all) aquaculture ponds in the coastal zones as tidal flats (Supplementary Fig. 14), and this misclassification resulted in considerable overestimation of tidal flat areas in the GICD¹². The spatial distribution of tidal flats from our dataset agreed with those from the GICD, but a close zoom-in visual comparison indicated the higher accuracy of our dataset compared with that of the GICD. In addition, we compared our annual maps of mangrove forests with the other available datasets (Supplementary Fig. 15). The mangrove forest areas from our dataset agreed well with those from recent maps at the provincial scale, which were also derived from analysis of Landsat

images^{18–20} (Supplementary Note 5). Inter-comparison of tidal flat and mangrove forest areas from our dataset and the other datasets clearly shows the high accuracy and potential value of ours for analysis of coastal wetland dynamics over the past decades at an annual temporal resolution.

Sources of errors and uncertainties in coastal wetland maps. Our study, together with previous works^{3,12,15,16,19–21}, has contributed to the current study of coastal wetlands in China. However, we must also recognize the sources of errors and uncertainties in the annual coastal wetland maps, which helps us to understand the caveats associated with this study and to identify the path forward for further improvement of coastal wetland maps in the near future. Because the spatial resolution of Landsat is 30 m, some coastal wetlands of areas $< 30 \times 30 \text{ m}^2$ could not be identified or mapped. The number of images of China's coastal provinces was lower in 2012 than in 2000–2011 and 2013–2018 (Supplementary Fig. 16), which might have contributed to the low coastal wetland areas recorded in 2012, especially widely distributed tidal flats (Supplementary Fig. 17). However, the percentage of pixels with a number of good observations of 0 was much higher in 2013–2018, and coastal wetland area estimates during the period 2013–2018 had high confidence. Because additional historical Landsat data will be added to the GEE platform by the USGS Landsat Global Archive Consolidation, more Landsat images are likely to further improve the accuracy of coastal wetland maps in the future.

Accurate high-tide lines are critical for the accuracy of the resultant coastal wetland areas^{12,15}. However, the high-tide line under closed-canopy tidal vegetation is different from that detected using Landsat images. In this study, we used artificial shorelines to define the scope of coastal wetlands. Because of the uncertainties of artificial shorelines delineated using visual interpretation, some inland vegetation located between artificial shorelines and seawater could have been included in this study and misidentified as tidal vegetation. In the near future, open-access optical and microwave images could be combined to detect high-tide lines and improve the accuracy of the resultant wetland maps.

Statistical analyses. Inter-annual variation and trends in coastal wetland areas for the period 1984–2018 at different spatial scales were calculated and analysed through linear regression models with a *t*-test at the 5% significance level. Coastal wetland areas within 1-km grid cells for China were summed in each 30-m map for the period 1984–2018, and their inter-annual variation and trends were also calculated and analysed through simple linear regression models. Additionally, we explored the relationship of tidal vegetation and tidal flat areas with other drivers using simple linear regression and multiple linear regression models. Linear regression models were carried out using the 'lm' function in R code (<https://www.rdocumentation.org/packages/stats/versions/3.6.2/topics/lm>).

Structural equation modelling (SEM) was also used to analyse driving factors for coastal wetland dynamics in China. SEM can investigate multiple related and dependent variables simultaneously, estimate the structure and relationship of variables simultaneously and estimate the fitting degree of the model as a whole. In the multiple linear regression model and SEM, the variance inflation factor (VIF) of each variable was calculated: when $VIF \geq 10$, the factor was not included in the model. SEM analysis was carried out using the 'piecewiseSEM' statistical package in R code (<https://cran.r-project.org/web/packages/piecewiseSEM/vignettes/piecewiseSEM.html>).

Reporting Summary. Further information on research design is available in the Nature Research Reporting Summary linked to this article.

Data availability

All datasets used in this study are publicly available online (Supplementary Table 7). The coastal wetlands maps are available from the corresponding author upon reasonable request and will be made available to the public. Source data are provided with this paper.

Code availability

The codes used in the calculations of coastal wetlands are available upon reasonable request.

Received: 20 October 2020; Accepted: 27 September 2021;

Published online: 28 October 2021

References

1. Ma, Z. J. et al. Rethinking China's new great wall. *Science* **346**, 912–914 (2014).
2. Murray, N. J. et al. The global distribution and trajectory of tidal flats. *Nature* **565**, 222–225 (2019).
3. Wang, X. et al. Tracking annual changes of coastal tidal flats in China during 1986–2016 through analyses of Landsat images with Google Earth Engine. *Remote Sens. Environ.* **238**, 110987 (2020).
4. Blum, M. D. & Roberts, H. H. Drowning of the Mississippi Delta due to insufficient sediment supply and global sea-level rise. *Nat. Geosci.* **2**, 488–491 (2009).

5. Murray, N. J., Clemens, R. S., Phinn, S. R., Possingham, H. P. & Fuller, R. A. Tracking the rapid loss of tidal wetlands in the Yellow Sea. *Front. Ecol. Environ.* **12**, 267–272 (2014).
6. Gedan, K. B., Silliman, B. R. & Bertness, M. D. Centuries of human-driven change in salt marsh ecosystems. *Ann. Rev. Mar. Sci.* **1**, 117–141 (2009).
7. Syvitski, J. P. M., Vörösmarty, C. J., Kettner, A. J. & Green, P. Impact of humans on the flux of terrestrial sediment to the global coastal ocean. *Science* **308**, 376–380 (2005).
8. Cui, B., He, Q., Gu, B., Bai, J. & Liu, X. China's coastal wetlands: understanding environmental changes and human impacts for management and conservation. *Wetlands* **36**, 1–9 (2016).
9. Gong, P. et al. Stable classification with limited sample: transferring a 30-m resolution sample set collected in 2015 to mapping 10-m resolution global land cover in 2017. *Sci. Bull.* **64**, 370–373 (2019).
10. Han, Q., Niu, Z., Wu, M. & Wang, J. Remote-sensing monitoring and analysis of China intertidal zone changes based on tidal correction. *Sci. Bull.* **64**, 456–473 (2019).
11. Mao, D. et al. National wetland mapping in China: a new product resulting from object-based and hierarchical classification of Landsat 8 OLI images. *ISPRS J. Photogramm. Remote Sens.* **164**, 11–25 (2020).
12. Wang, X. et al. Mapping coastal wetlands of China using time series Landsat images in 2018 and Google Earth Engine. *ISPRS J. Photogramm. Remote Sens.* **163**, 312–326 (2020).
13. Mcowen, C. J. et al. A global map of saltmarshes. *Biodivers. Data J.* **5**, e11764 (2017).
14. Giri, C. et al. Status and distribution of mangrove forests of the world using Earth observation satellite data. *Glob. Ecol. Biogeogr.* **20**, 154–159 (2011).
15. Chen, Y. et al. Effects of reclamation and natural changes on coastal wetlands bordering China's Yellow Sea from 1984 to 2015. *Land Degrad. Dev.* **30**, 1533–1544 (2019).
16. Hu, Y. et al. Mapping coastal salt marshes in China using time series of Sentinel-1 SAR. *ISPRS J. Photogramm. Remote Sens.* **173**, 122–134 (2021).
17. Zhang, X. et al. Quantifying expansion and removal of *Spartina alterniflora* on Chongming Island, China, using time series Landsat images during 1995–2018. *Remote Sens. Environ.* **247**, 111916 (2020).
18. Chen, B. Q. et al. A mangrove forest map of China in 2015: analysis of time series Landsat 7/8 and Sentinel-1A imagery in Google Earth Engine cloud computing platform. *ISPRS J. Photogramm. Remote Sens.* **131**, 104–120 (2017).
19. Hu, L., Li, W. & Xu, B. Monitoring mangrove forest change in China from 1990 to 2015 using Landsat-derived spectral-temporal variability metrics. *Int. J. Appl. Earth Obs. Geoinf.* **73**, 88–98 (2018).
20. Jia, M., Wang, Z., Zhang, Y., Mao, D. & Wang, C. Monitoring loss and recovery of mangrove forests during 42 years: the achievements of mangrove conservation in China. *Int. J. Appl. Earth Obs. Geoinf.* **73**, 535–545 (2018).
21. Jia, M. et al. Rapid, robust, and automated mapping of tidal flats in China using time series Sentinel-2 images and Google Earth Engine. *Remote Sens. Environ.* **255**, 112285 (2021).
22. Ma, T., Li, X., Bai, J. & Cui, B. Tracking three decades of land use and land cover transformation trajectories in China's large river deltas. *Land Degrad. Dev.* **30**, 799–810 (2019).
23. Wang, K. Evolution of Yellow River delta coastline based on remote sensing from 1976 to 2014, China. *Chin. Geogr. Sci.* **29**, 181–191 (2019).
24. Zhao, Y. F. et al. Assessing natural and anthropogenic influences on water discharge and sediment load in the Yangtze River, China. *Sci. Total Environ.* **607**, 920–932 (2017).
25. Yim, J. et al. Analysis of forty years long changes in coastal land use and land cover of the Yellow Sea: the gains or losses in ecosystem services. *Environ. Pollut.* **241**, 74–84 (2018).
26. Wang, S. et al. Reduced sediment transport in the Yellow River due to anthropogenic changes. *Nat. Geosci.* **9**, 38–41 (2016).
27. Chen, Y. et al. Land claim and loss of tidal flats in the Yangtze Estuary. *Sci. Rep.* **6**, 24018 (2016).
28. Yang, M. et al. Spatio-temporal characterization of a reclamation settlement in the Shanghai coastal area with time series analyses of X-, C-, and L-band SAR datasets. *Remote Sens.* **10**, 329 (2018).
29. Han, X., Pan, J. & Devlin, A. T. Remote sensing study of wetlands in the Pearl River Delta during 1995–2015 with the support vector machine method. *Front. Earth Sci.* **12**, 521–531 (2018).
30. Liu, L., Xu, W., Yue, Q., Teng, X. & Hu, H. Problems and countermeasures of coastline protection and utilization in China. *Ocean Coast. Manag.* **153**, 124–130 (2018).
31. Yunxuan, Z. et al. Degradation of coastal wetland ecosystem in China: drivers, impacts, and strategies. *Bull. Chin. Acad. Sci.* **31**, 1157–1166 (2016).
32. Jiang, T. T., Pan, J. F., Pu, X. M., Wang, B. & Pan, J. J. Current status of coastal wetlands in China: degradation, restoration, and future management. *Estuar. Coast. Shelf Sci.* **164**, 265–275 (2015).
33. Sun, Z. et al. China's coastal wetlands: conservation history, implementation efforts, existing issues and strategies for future improvement. *Environ. Int.* **79**, 25–41 (2015).
34. Ren, C. et al. Rapid expansion of coastal aquaculture ponds in China from Landsat observations during 1984–2016. *Int. J. Appl. Earth Obs. Geoinf.* **82**, 101902 (2019).
35. Gu, J. et al. Losses of salt marsh in China: trends, threats and management. *Estuar. Coast. Shelf Sci.* **214**, 98–109 (2018).
36. Wang, W., Liu, H., Li, Y. & Su, J. Development and management of land reclamation in China. *Ocean Coast. Manag.* **102**, 415–425 (2014).
37. Barbier, E. B. et al. The value of estuarine and coastal ecosystem services. *Ecol. Monogr.* **81**, 169–193 (2011).
38. Barbier, E. B. A global strategy for protecting vulnerable coastal populations. *Science* **345**, 1250–1251 (2014).
39. He, Q. et al. Economic development and coastal ecosystem change in China. *Sci. Rep.* **4**, 5995 (2014).
40. Zhou, C. et al. Preliminary analysis of C sequestration potential of blue carbon ecosystems on Chinese coastal zone. *Sci. China Life Sci.* **46**, 475–486 (2016).
41. Zhang, Q. et al. Propagule types and environmental stresses matter in saltmarsh plant restoration. *Ecol. Eng.* **143**, 105693 (2020).
42. Cui, B., Yang, Q., Yang, Z. & Zhang, K. Evaluating the ecological performance of wetland restoration in the Yellow River Delta, China. *Ecol. Eng.* **35**, 1090–1103 (2009).
43. Pan, X. Research on Xi Jinping's thought of ecological civilization and environment sustainable development. *IOP Conf. Ser. Earth Environ. Sci.* **153**, 062067 (2018).
44. Hansen, M. H., Li, H. & Svarverud, R. Ecological civilization: interpreting the Chinese past, projecting the global future. *Glob. Environ. Change.* **53**, 195–203 (2018).
45. Moreno-Mateos, D., Power, M. E., Comin, F. A. & Yockteng, R. Structural and functional loss in restored wetland ecosystems. *PLoS Biol.* **10**, e1001247 (2012).
46. He, Q. Conservation: 'No net loss' of wetland quantity and quality. *Curr. Biol.* **29**, R1070–R1072 (2019).
47. Gong, P., Li, X. & Zhang, W. 40-year (1978–2017) human settlement changes in China reflected by impervious surfaces from satellite remote sensing. *Sci. Bull.* **64**, 756–763 (2019).
48. Wang, X. et al. Gainers and losers of surface and terrestrial water resources in China during 1989–2016. *Nat. Commun.* **11**, 3471 (2020).
49. Zou, Z. H. et al. Divergent trends of open-surface water body area in the contiguous United States from 1984 to 2016. *Proc. Natl Acad. Sci. USA* **115**, 3810–3815 (2018).

Acknowledgements

X.W., B.L. and X. Xu were supported by the National Natural Science Foundation of China (grant nos. 41630528 and 32030067). X. Xiao and Y.Q. were supported by the US National Science Foundation (grant no. 1911955). X.W. and X. Xu were supported by the China Postdoctoral Science Foundation (grant nos. 2021TQ0072, BX20200094 and 2020M681164). L.P. was supported by the Natural Science Foundation of Guangxi Province (grant no. 2017GXNSFBA198009). X.W. was supported by the China Scholarship Council (grant no. 201906100124). We thank Q. He from Fudan University for discussions and literature that helped improve the Discussion section of the manuscript.

Author contributions

X. Xiao, X.W. and B.L. designed the study. X.W. carried out image data processing. X.W., X. Xiao and B.L. led interpretation of the results and writing of the manuscript. Z.Z., B.C., Y.Q., X.Z., J.D. and D.L. contributed to image data processing. X. Xu, Y.Q., X.Z., J.D. and L.P. contributed to interpretation and discussion of results.

Competing interests

The authors declare no competing interests.

Additional information

Supplementary information The online version contains supplementary material available at <https://doi.org/10.1038/s41893-021-00793-5>.

Correspondence and requests for materials should be addressed to Xiangming Xiao or Bo Li.

Peer review information *Nature Sustainability* thanks Andrea Ghermandi and the other, anonymous, reviewer(s) for their contribution to the peer review of this work.

Reprints and permissions information is available at www.nature.com/reprints.

Publisher's note Springer Nature remains neutral with regard to jurisdictional claims in published maps and institutional affiliations.

© The Author(s), under exclusive licence to Springer Nature Limited 2021

Reporting Summary

Nature Portfolio wishes to improve the reproducibility of the work that we publish. This form provides structure for consistency and transparency in reporting. For further information on Nature Portfolio policies, see our [Editorial Policies](#) and the [Editorial Policy Checklist](#).

Statistics

For all statistical analyses, confirm that the following items are present in the figure legend, table legend, main text, or Methods section.

n/a Confirmed

- The exact sample size (n) for each experimental group/condition, given as a discrete number and unit of measurement
- A statement on whether measurements were taken from distinct samples or whether the same sample was measured repeatedly
- The statistical test(s) used AND whether they are one- or two-sided
Only common tests should be described solely by name; describe more complex techniques in the Methods section.
- A description of all covariates tested
- A description of any assumptions or corrections, such as tests of normality and adjustment for multiple comparisons
- A full description of the statistical parameters including central tendency (e.g. means) or other basic estimates (e.g. regression coefficient) AND variation (e.g. standard deviation) or associated estimates of uncertainty (e.g. confidence intervals)
- For null hypothesis testing, the test statistic (e.g. F , t , r) with confidence intervals, effect sizes, degrees of freedom and P value noted
Give P values as exact values whenever suitable.
- For Bayesian analysis, information on the choice of priors and Markov chain Monte Carlo settings
- For hierarchical and complex designs, identification of the appropriate level for tests and full reporting of outcomes
- Estimates of effect sizes (e.g. Cohen's d , Pearson's r), indicating how they were calculated

Our web collection on [statistics for biologists](#) contains articles on many of the points above.

Software and code

Policy information about [availability of computer code](#)

Data collection

Data analysis

For manuscripts utilizing custom algorithms or software that are central to the research but not yet described in published literature, software must be made available to editors and reviewers. We strongly encourage code deposition in a community repository (e.g. GitHub). See the Nature Portfolio [guidelines for submitting code & software](#) for further information.

Data

Policy information about [availability of data](#)

All manuscripts must include a [data availability statement](#). This statement should provide the following information, where applicable:

- Accession codes, unique identifiers, or web links for publicly available datasets
- A description of any restrictions on data availability
- For clinical datasets or third party data, please ensure that the statement adheres to our [policy](#)

Field-specific reporting

Please select the one below that is the best fit for your research. If you are not sure, read the appropriate sections before making your selection.

Life sciences Behavioural & social sciences Ecological, evolutionary & environmental sciences

For a reference copy of the document with all sections, see [nature.com/documents/nr-reporting-summary-flat.pdf](https://www.nature.com/documents/nr-reporting-summary-flat.pdf)

Ecological, evolutionary & environmental sciences study design

All studies must disclose on these points even when the disclosure is negative.

Study description	This study quantified the spatial-temporal dynamics of coastal wetlands in China and investigated the relative contributions of the driving factors to the coastal wetland changes during 1984-2018.
Research sample	This study does not contain research samples in the fields. For Landsat image analysis, we collected samples of pixels for algorithm calibration and map accuracy assessment.
Sampling strategy	For Landsat image analysis, stratified and random sampling strategy was used.
Data collection	1. all the available Landsat 5/7/8 Surface Reflectance images during 1984-2018 (~62,000 images) in Google Earth Engine cloud computing platform 2. annual coastal wetland maps in China from the analysis of Landsat images during 1984-2018. 3. main driving factors (sea level rise, urbanization, population, GDP, sediment flux changes, construction of national nature reserves, and government policies and laws) in China during 1984-2018.
Timing and spatial scale	The start and end dates of this collection is 1984/01/01-2018/12/31, and the spatial resolution is 30-m. Because of the limited number of good-quality observations within a year during 1984-1989, we generated the coastal wetland maps within each three-year time-period (1984-1986 and 1987-1989), for example, we generated the maps of 1985 using all Landsat data during 1984-1986. Therefore, in this study we generated two 3-year maps (1985 and 1988) and twenty-nine annual maps of coastal wetlands during 1990-2018, making a total of 31 maps.
Data exclusions	Bad-quality observations in Landsat images.
Reproducibility	Landsat image analyses were performed in the Google Earth Engine cloud computing platform, and they could be reproduced by researchers through this platform. Statistical analyses can also be reproduced.
Randomization	No randomization in the parameters of the mapping algorithms and the mapping procedure.
Blinding	No blinding in the mapping procedure.
Did the study involve field work?	<input type="checkbox"/> Yes <input checked="" type="checkbox"/> No

Reporting for specific materials, systems and methods

We require information from authors about some types of materials, experimental systems and methods used in many studies. Here, indicate whether each material, system or method listed is relevant to your study. If you are not sure if a list item applies to your research, read the appropriate section before selecting a response.

Materials & experimental systems

n/a	Involvement in the study
<input checked="" type="checkbox"/>	<input type="checkbox"/> Antibodies
<input checked="" type="checkbox"/>	<input type="checkbox"/> Eukaryotic cell lines
<input checked="" type="checkbox"/>	<input type="checkbox"/> Palaeontology and archaeology
<input checked="" type="checkbox"/>	<input type="checkbox"/> Animals and other organisms
<input checked="" type="checkbox"/>	<input type="checkbox"/> Human research participants
<input checked="" type="checkbox"/>	<input type="checkbox"/> Clinical data
<input checked="" type="checkbox"/>	<input type="checkbox"/> Dual use research of concern

Methods

n/a	Involvement in the study
<input checked="" type="checkbox"/>	<input type="checkbox"/> ChIP-seq
<input checked="" type="checkbox"/>	<input type="checkbox"/> Flow cytometry
<input checked="" type="checkbox"/>	<input type="checkbox"/> MRI-based neuroimaging